Hindawi
Geofluids
Volume 2022, Article ID 7929351, 8 pages
https://doi.org/10.1155/2022/7929351

Research Article

Sequence Stratigraphy Variation and Its Implication in Shale Oil Exploration: A Case Study of the Eocene Dongying Depression, Eastern China

Jing Wu,[1,2] **Wei Li**,[1,2] **Wenjin Li**,[1,2] **and Wei Chen**[1,2]

[1]*School of Earth Science and Engineering, Shandong University of Science and Technology, Qingdao 266590, China*
[2]*Shandong Province Key Laboratory of Depositional Mineralization & Sedimentary Mineral, Shandong University of Science and Technology, Qingdao 266590, China*

Correspondence should be addressed to Jing Wu; wujing6524982@163.com and Wei Li; lw1630305@163.com

Received 10 February 2022; Accepted 8 April 2022; Published 25 April 2022

Academic Editor: Wenming Ji

Copyright © 2022 Jing Wu et al. This is an open access article distributed under the Creative Commons Attribution License, which permits unrestricted use, distribution, and reproduction in any medium, provided the original work is properly cited.

Organic matter (OM) and carbonate are the important organic and inorganic components, respectively, in the shales of the upper fourth member of the Eocene Shahejie Formation, Dongying Depression, Eastern China. Their enrichment affects the hydrocarbon generation capacity and reservoir development of shales. The development mechanism of sequence stratigraphy and the influence of sequence stratigraphy on OM enrichment and carbonate deposition are investigated in this study. Based on the petrological, mineralogical, and geochemical analyses, a third-order sequence is recognized, including the lowstand systems tract (LST), transgressive systems tract (TST), and highstand systems tract (HST). The total organic carbon (TOC) content is 0.11–9.05 wt% (average 2.2 wt%), and the carbonate content is 3–95 wt% (average 51 wt%). Organic matter and carbonate are enriched in TST and gradually reduced in HST and LST. The decrease in the relative lake level in LST results in the deposition of abundant siltstone, leading to both poor OM preservation and carbonate precipitation. The rapid rise in the relative lake level in TST may be triggered by marine transgression, promoting OM enrichment in terms of both production and preservation. Seawater input brought abundant Ca^{2+} and Mg^{2+}, which facilitated the precipitation of carbonates. The enrichment of OM and carbonate improves the capacity of hydrocarbon generation and reservoir performance of shales in the TST. The decrease in the relative lake level in HST causes a slight increase in the terrigenous clastic content, which, on the one hand, accelerates the sedimentation rate and OM deposition and, on the other hand, reduces carbonate precipitation. This study not only explains the differential distribution of OM and carbonate but also helps to improve the accuracy of the evaluation of shale oil sweet spots.

1. Introduction

Sequence stratigraphy was proposed some 30 years ago with the publications of Society for Sedimentary Geology (SEPM) Special Publication 42 and the American Association of Petroleum Geologists (AAPG) Methods in Exploration Series No. 7 [1, 2]. It has been used successfully in passive continental margin environments and lacustrine basins [3–7]. In recent years, with the exploration and development of shale oil and gas, a large number of studies on sequence stratigraphy have been carried out for shales [5, 7]. Three main methods have been applied to the identification of the sequence stratigraphic framework. (1) Apply mineral composition and petrological variation to identify sequence stratigraphic boundaries and units. The type and variation of mineral compositions and lithofacies are influenced by relative sea/lake level fluctuations and thus can be used as indicators for establishing sequence stratigraphic frameworks [8, 9]. (2) Apply geochemical indicators to establish a sequence stratigraphic framework. Inorganic geochemical indicators mainly include Th/U, V/(V + Ni), and Cr/Al ratios, and organic geochemical indicators mainly include total organic carbon (TOC) content and relative hydrocarbon potential [10, 11]. (3) Establish a

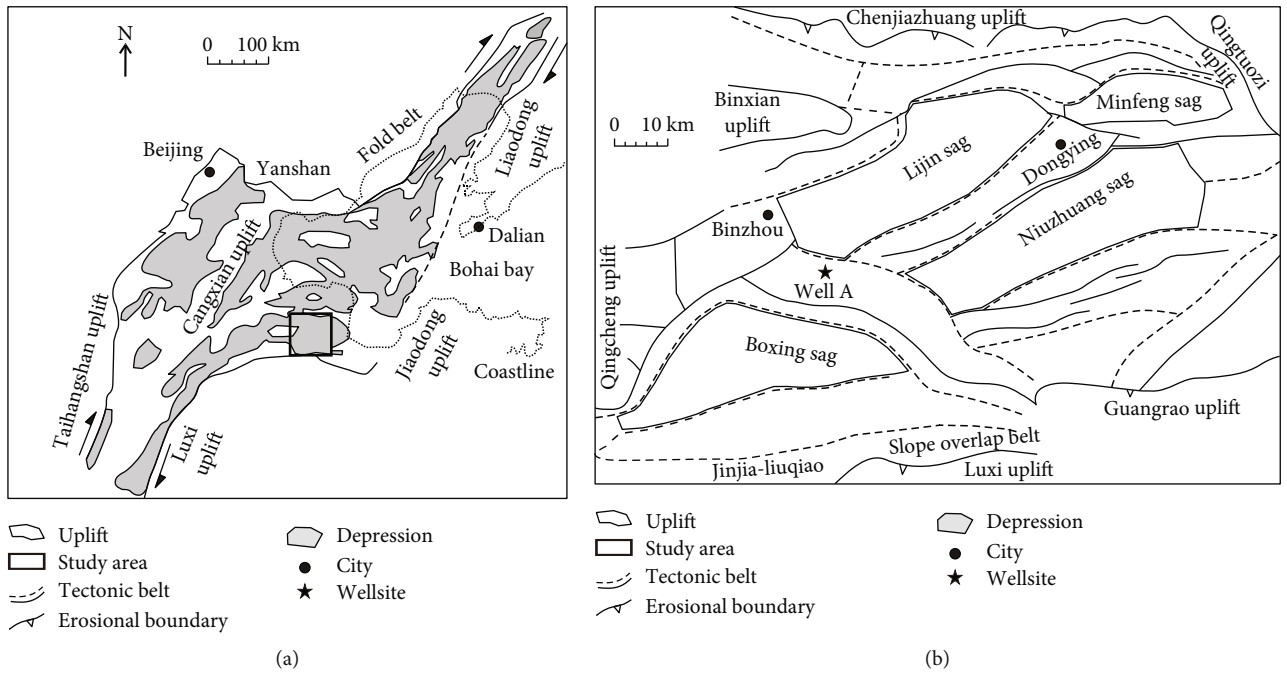

Figure 1: Geological background of the Es4u shale within the Dongying Depression. (a) Location of the Dongying Depression, Bohai Bay Basin, Eastern China. (b) Structural map of the Dongying Depression, including the position of the wellsite [21, 24].

sequence stratigraphic framework using logging data [12, 13]. The gamma curve reaches a maximum at the maximum flood surface [11]. Compared with marine shales, lacustrine shales have a small depositional scale, large spatial and temporal variability, complex mineralogical composition, and diverse depositional processes, which lead to the complexity and specificity of sequence stratigraphy of lacustrine shales. Thus, the sequence stratigraphy of lacustrine shales needs further study [14]. In addition, organic matter (OM) is an important component of shale [15]. It influences the deposition and diagenesis of minerals (i.e., carbonate, clay minerals, and feldspar) and the formation of shale reservoirs [16, 17]. Carbonate is one of the important minerals of lacustrine shales in China (average 65 wt%) and influences reservoir and hydraulic fracturing of shale formations [18, 19]. Studying the influence of sequence stratigraphy on OM enrichment and carbonate deposition is helpful for stratigraphic comparison and prediction of the distribution of shale oil and gas sweet spots.

The Dongying Depression has the most abundant oil and gas resources in the Cenozoic fault basin in Eastern China. The upper fourth member of the Eocene Shahejie Formation (Es4u) is a prolific source rock interval, which has become a significant exploration target for shale oil in recent years [19–21]. Well A within the Dongying Depression covers nearly 200 m of lacustrine organic-rich shale, providing an excellent opportunity to study the sequence stratigraphy. This study will help in understanding the mechanism of source rock quality differences in a sequence stratigraphic context, which is of significance for improving the accuracy of the evaluation of source rocks and shale oil resources.

2. Geological Background

Developed as a result of the Tertiary rifting, the Dongying Depression is located at the southeastern corner of the Bohai Bay Basin in China (Figure 1(a)) [22], with an area of 5700 km^2. It is surrounded by the Luxi uplift to the south, Chenjiazhuang uplift to the north, Qingtuozi uplift to the east, and Binxian-Qingcheng uplift to the west (Figure 1 (b)) [19]. The Dongying Depression is subdivided into four sags: the Boxing, Niuzhuang, Lijin, and Minfeng sags. The tectonic evolution of the Dongying Depression consists of a rifting stage, a fault-depression conversion stage, and a thermal subsidence stage. The rifting stage is subdivided into three phases (Figure 2).

The Dongying Depression comprises a Cenozoic rift basin stratum, which is composed of the Paleogene Kongdian, Shahejie (Es), and Dongying formations, the Neogene Guantao and Minghuazhen formations, and the Quarternary Pingyuan Formation [23]. These formations are dominated by fluvial, delta, and lacustrine deposits (Figure 2). The Es Formation can be further subdivided into four members: Es4, Es3, Es2, and Es1 members (Figure 2). The lower member of the Es4 (Es4l) is characterized by fine sandstones, siltstones, and red mudstones. Dark gray shales are developed in the middle and upper parts of the Es4u member, and gray siltstones are developed in the lower part [23].

3. Methods

A total of 368 samples were collected from Well A in this study (sampling depths from 3450 to 3251 m; see Figure 1 (b) for the location). Samples were taken at 0.5 m intervals. Detailed analyses of minerals, petrology, Rock-Eval

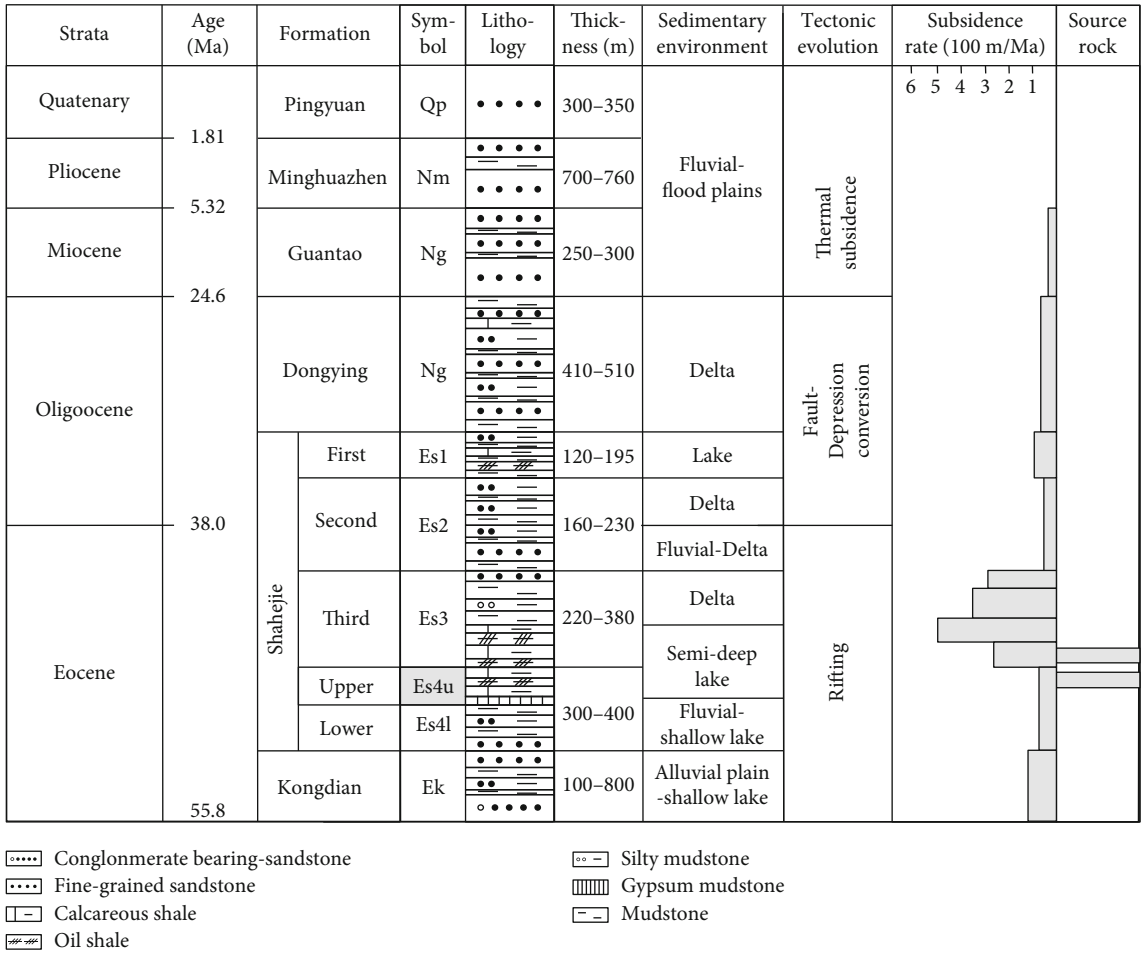

Figure 2: Stratigraphic column of the Dongying Depression (modified from [22]).

pyrolysis, and multiple geochemical proxies were performed. All tests were conducted at the Geoscience Institute of the Shengli Oilfield, SINOPEC.

Trace elements (Fe, Al, etc.) analyses were conducted on 49 powdered samples with inductively coupled plasma atomic emission spectrometry (ICP-AES). The relative standard deviation was less than 4%. TOC analysis was done on 93 samples by a CS344 carbon-sulfur analyzer (LECO Company, US). These samples were also analyzed for Rock-Eval pyrolysis tests to determine the free hydrocarbons (S1, mg HC/g rock), hydrocarbons generated from kerogen (S2, mg HC/g rock), and temperature of the maximum S2 yield (T_{max}). A total of 368 samples were collected for the whole-rock X-ray diffraction (XRD) analysis. This analysis was conducted by a Bruker D8 DISCOVER automatic powder XRD analyzer. Thin section examination using a polarizing Zeiss microscope was completed on 36 samples. Natural gamma spectroscopy logging data (including K, Th, and U) was collected for the sequence stratigraphic analysis.

4. Results

4.1. Petrological Characteristics. We identified four major lithofacies in the Es4u member based on mineral compositions and sedimentary structures: calcareous shale, mixed shale, clayey shale, and siltstone (Figure 3). The clayey shale (clay mineral content > 50 wt%) and the siltstone (silt content > 50 wt%) are limited to the lower part of the Es4u member. The laminae are developed in the clayey shale, while cross-bedding and massive bedding are developed in the siltstone (Figures 3(a) and 3(b)). The calcareous shale and mixed shale are the most common lithofacies, which are distributed in the middle and upper parts of the Es4u shale, respectively (Figures 3(c)–3(f)). The laminae are both developed in these two lithofacies. The carbonate content of the calcareous shale is more than 50% (Figure 3(c)), while the carbonate content, siliceous mineral content, and clay mineral content of the mixed shale are approximately similar (Figure 3(f)).

4.2. Mineralogical Characteristics. Carbonates are the most abundant mineral in the Es4u shale (Figure 4). The carbonate content is 3–95 wt%, with an average of 51 wt%. Carbonates are composed of calcite (average 38 wt%), dolomite (average 14 wt%), and siderite (average 1 wt%). The remaining inorganic compositions of the Es4u shale are mainly quartz, clay minerals (illite, kaolinite, chlorite, and illite/smectite mixed layers), and feldspar. Quartz content ranges

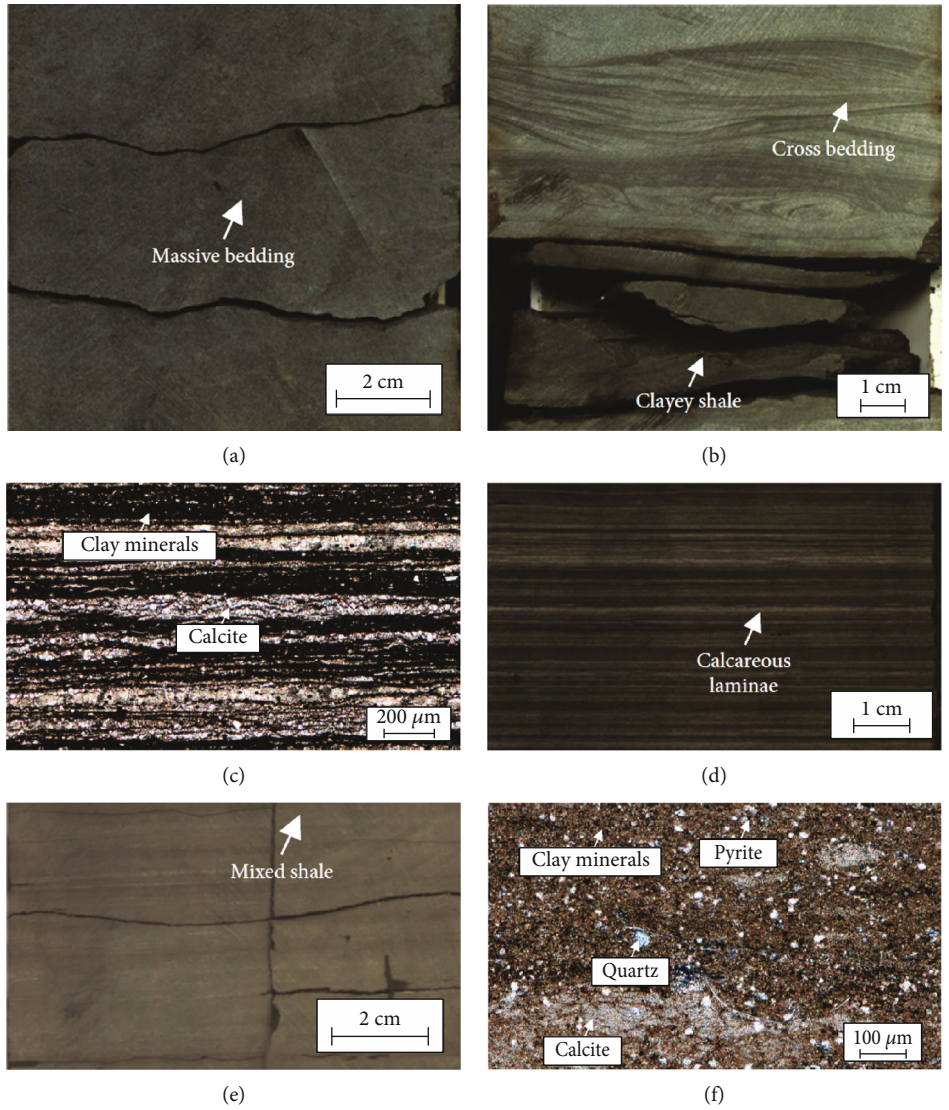

Figure 3: Characteristics of main lithofacies in the Es4u member in the Dongying Depression. (a) Massive bedding developed in the siltstone, 3439 m. (b) Gray clayey shale and cross-bedding developed in the siltstone, 3444 m. (c) Calcareous shale: light laminae comprise calcite; dark laminae are composed of clay minerals, 3397.5 m. (d) Dark gray calcareous shale developing dark and light laminae, 3397.5 m. (e) Gray mixed shale developing laminae, 3331.5 m. (f) Mixed shale composed of calcite, quartz, clay minerals, and pyrite, 3331.5 m.

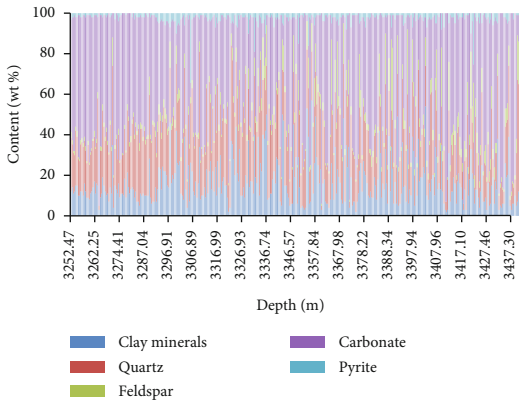

Figure 4: The main mineral contents of the Es4u shale in the Dongying Depression.

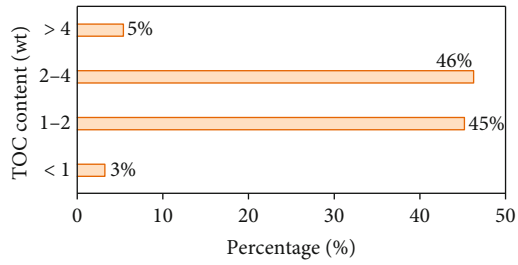

Figure 5: The distribution of the TOC content in the Es4u shale in the Dongying Depression.

from 2 to 60 wt%, with an average of 24 wt%. Clay mineral content is 2–57 wt% (average 16 wt%). In addition, a very small amount of gypsum is found in the Es4u shale.

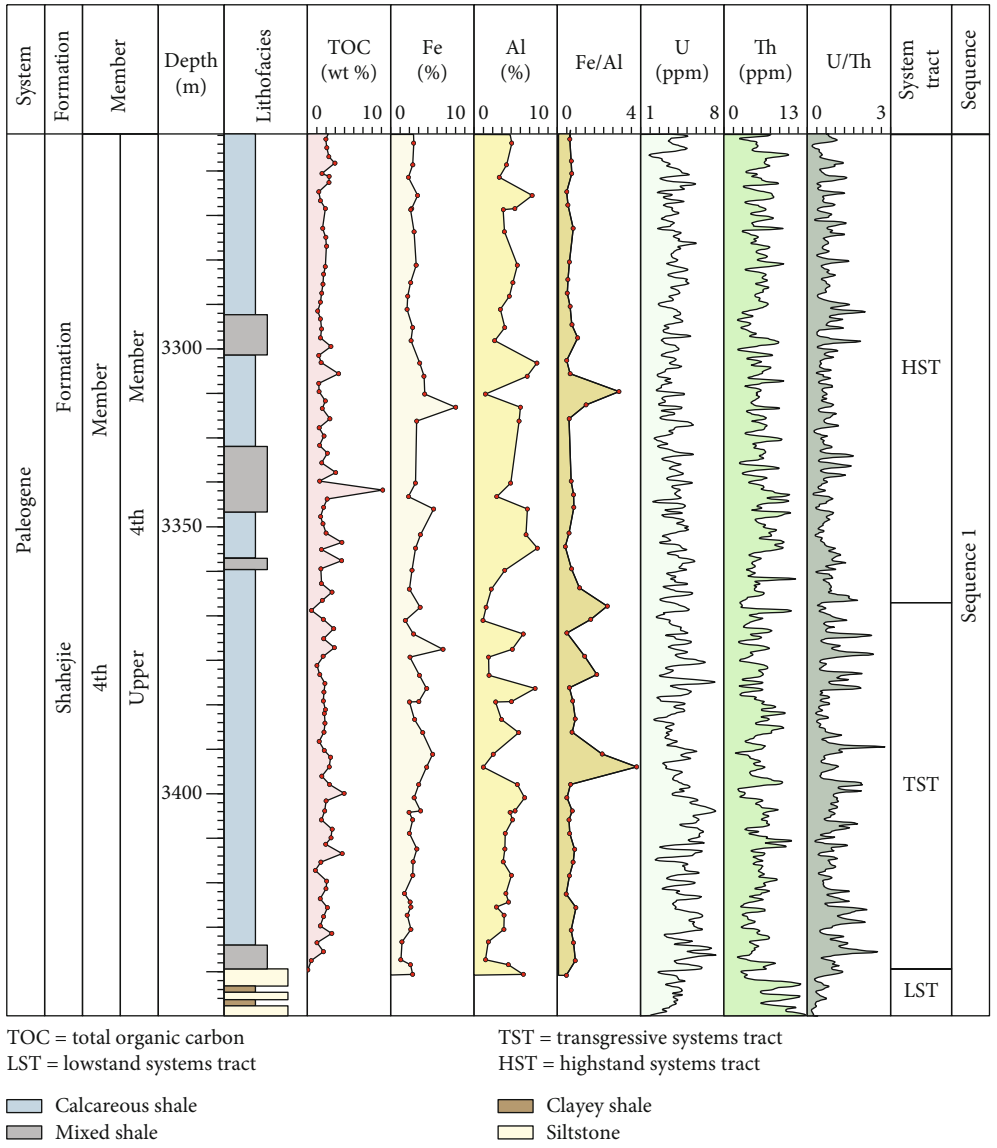

Figure 6: Geochemical parameters and sequence stratigraphy of the Es4u shale in Well A in the Dongying Depression.

4.3. Geochemical Parameters. The TOC content of 93 samples ranges from 0.11 to 9.05 wt%, with an average of 2.2 wt%. Among them, most of the samples have a TOC content between 1 and 4 wt% (Figure 5). Only 3% of the samples have a TOC content of less than 1 wt%. Thus, the Es4u shale as a whole is rich in OM. The U content ranges from 1.71 to 7.33 ppm, with an average of 4.04 ppm, and the Th content is in the range of 1.77–14.98 ppm (average 5.72 ppm, Figure 6). The U/Th ratio ranges from 0.36 to 8.01 (average 1.55). The Fe content varies between 1.20 and 7.72% (average 2.97%), and the Al content varies between 1.08% and 7.61% (average 4.11%, Figure 6). The Fe/Al ratio ranges from 0.39 to 3.81 (average 0.90).

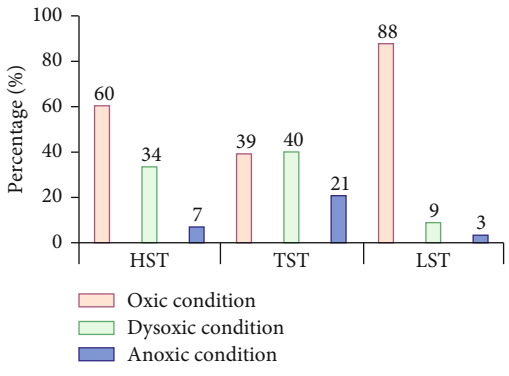

Figure 7: The sequence stratigraphic distribution of U/Th ratios in the Es4u member in the Dongying Depression.

5. Discussion

5.1. Sequence Stratigraphic Framework. Based on the above petrological and geochemical characteristics, a third-order sequence in the Es4u member has been recognized, compris-

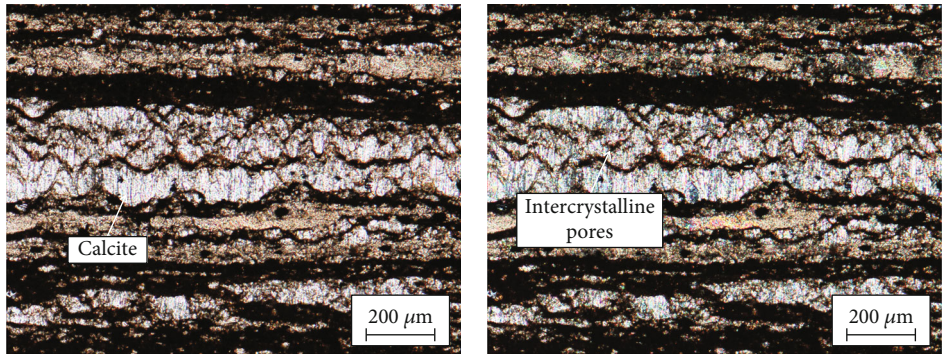

(a) (b)

Figure 8: Characteristics of intercrystalline pores in the Es4u shale in the Dongying Depression. (a) Recrystallized intercrystalline pores. During the recrystallization process of calcite, the crystal volume becomes smaller, thus forming recrystallized intercrystalline pores. (-), 3397.5 m. (b) Recrystallized intercrystalline pores. The pore size is about 10 μm, and some of the pores are filled with oil. (+), 3397.5 m.

ing the lowstand systems tract (LST), transgressive systems tract (TST), and highstand systems tract (HST) (Figure 6).

5.1.1. Lowstand Systems Tract (3439-3450 m). The bottom boundary of the LST is also the bottom boundary of the Es4u member. This boundary separates the Es4u member from the Es4l member characterized by the red mudstone. Gray siltstone is dominantly developed in the LST and has been interpreted as a beach bar deposition in the shallow lake based on the sedimentary structures (cross-bedding, massive bedding, etc.) and lithofacies combination [23, 25]. The top boundary of the LST is the initial flooding surface [3]. Additionally, elements (such as uranium and thorium) are sensitive to changes in redox conditions of bottom water and are widely applied in sequence stratigraphy research [10, 26, 27]. U/Th < 0.75 indicates an oxic condition, 0.75 < U/Th < 1.25 suggests a dysoxic condition, and U/Th > 1.25 represents an anoxic condition [28]. During the LST, the U/Th ratio is consistently low between 0.15 and 1.27, with a mean value of only 0.49. 88% of the U/Th ratios are less than 0.75. The petrological and geochemical characteristics in the LST suggest an oxic condition in the shallow lake (Figure 7).

5.1.2. Transgressive Systems Tract (3357-3439 m). The TST begins after the initial flooding surface [3]. The siltstone is no longer developed in the TST. The development of abundant calcareous shales indicates that the lake basin is less influenced by terrigenous input. The development of stable laminae in the calcareous shale suggests a quiet water body in the lake basin. Fe (ferrum) and Al (aluminum) are also sensitive to redox conditions of bottom water [26, 29]. The Fe/Al ratio is an effective proxy for bottom-water redox conditions and is positively proportional to the redox potential [26, 29, 30]. Within the TST, the Fe/Al ratio ranges from 0.43 to 3.81 and the U/Th ratio ranges from 0.27 to 2.80. The mean values of Fe/Al and U/Th ratios increase to the maximum (1.03 and 0.95, respectively), indicating a continuous deepening of the water body to the maximum. In particular, 40% of the U/Th ratios indicate a dysoxic condition and 39% of the U/Th ratios indicate an anoxic condition (Figure 7). Eventually, the maximum flooding surface develops at the end of the TST.

5.1.3. Highstand Systems Tract (3251-3357 m). Alternation of calcareous shale and mixed shale occurs in the HST. Compared with the TST, the relative enrichment of siliciclastics (quartz, clay minerals, etc.) indicates an increased influence of terrigenous input in the HST. The Fe/Al ratio ranges from 0.39 to 2.96, and the U/Th ratio ranges from 0.17 to 2.08. The values of Fe/Al and U/Th are 0.77 and 0.73 on average, respectively. The Fe/Al and U/Th ratios show a decreasing trend upward, indicating an increased oxygen concentration and a decrease in the relative lake level.

5.2. The Influence of Sequence Stratigraphy on OM Enrichment. Two fundamental models have been established for OM enrichment: (1) the paleoproductivity model (i.e., phytoplankton blooms) [31, 32] and (2) the preservation model (i.e., bottom-water redox conditions) [33, 34]. During the TST, rapid deepening of the water body may be related to a marine transgression and warm-humid climate condition, which is inferred from the petrological and geochemical characteristics [35]. Seawater input not only raises the relative lake level and enhances the redox potential of bottom water but also brings nutrients and increases paleoproductivity. This satisfies the conditions for OM enrichment in terms of both the paleoproductivity and preservation conditions. The enrichment of OM can improve the capacity of hydrocarbon generation in shale. Moreover, during the evolution of OM, a large number of organic pores are developed within OM, which can provide pore space and permeation channels for shale oil [17, 21, 36, 37]. Therefore, OM enrichment in the TST is beneficial not only to the generation of shale oil but also to the storage of shale oil. In contrast, the relatively strong hydrodynamic force and oxic environment of the shallow lake in the LST are not conducive to the preservation of OM. The relative enrichment of terrigenous clastics in the HST accelerates the sedimentation rate. This results in the rapid accumulation and enrichment of OM [38]. Moreover, the terrigenous input in the HST is not as strong as that in the LST; otherwise, the OM will be difficult to preserve as in the LST.

5.3. The Influence of Sequence Stratigraphy on Carbonate Deposition. The analysis of mineralogical characteristics, occurrence, isotopes, electron probes, and element geochemistry suggest that the calcite in the study area is derived from chemical precipitation and photosynthesis of planktonic algae [18, 19, 39]. During the TST, the lack of terrigenous clastics and warm climate conditions are favorable for the deposition of carbonate [39, 40]. Additionally, seawater input brought abundant Ca^{2+} and Mg^{2+}, which is conducive to carbonate precipitation [41]. The carbonate content is 4–94 wt%, with an average of up to 54 wt%. According to Section 5.2, OM is enriched in TST, which can catalyze carbonate minerals to form intercrystalline pores, providing abundant storage space for shale oil (Figure 8) [18]. In contrast, the deposition of large amounts of siltstone in the LST hinders carbonate precipitation, and the average content of carbonate is as low as 12 wt%. In the HST, a decrease in the relative lake level leads to an enhanced input of terrigenous clastics. The mean value of quartz increases from 21 wt% in TST to 27 wt% in HST, and the corresponding mean value of carbonate decreases from 54 wt% in TST to 50 wt% in HST. The reduction of carbonate content leads to the reduction of intercrystalline pores.

6. Conclusions

A third-order sequence is recognized in the Es4u member, Dongying Depression, Eastern China. It contains the lowstand systems tract (LST), transgressive systems tract (TST), and highstand systems tract (HST). Organic matter (OM) and carbonate (the most dominant minerals) are mainly enriched in the TST, followed by the HST and LST. The development of different sequence stratigraphic units affects the paleoproductivity and redox conditions of the bottom water, which further influences the production and preservation of OM. The development of sequence stratigraphy determines the enrichment of OM, which therefore affects the hydrocarbon generation and reservoir development of shales. The development of the stratigraphic units also impacts the distribution and variation of carbonate deposition. Combined with the catalytic effect of OM on carbonates during diagenesis, the development of sequence stratigraphy further affects the formation of intercrystalline pores of carbonate, providing abundant storage space for shale oil. This study helps to understand the sedimentary environment and identify the spatial and temporal distribution pattern of high-quality shale reservoirs in the Eocene Dongying Depression.

Data Availability

Data are available on request.

Conflicts of Interest

There are no conflicts of interest concerning the results of this paper.

Acknowledgments

The results discussed in this paper were supported by the Natural Science Foundation of Shandong Province (No. ZR2019BD042), the National Natural Science Foundation of China (No. 41902134 and No. 42172165), and the China Postdoctoral Science Foundation Grant (No. 2019M652435 and No. 2020T130384).

References

[1] C. K. Wilgus, B. S. Hastings, C. G. Kendall et al., *Sea–Level Changes: An Integrated Approach*, vol. 42, Society for Sedimentary Geology, Tulsa, Oklahoma, 1988.

[2] J. C. Van Wagoner, R. M. Mitchum Jr., K. M. Campion, and V. D. Rahmanian, "Siliciclastic sequence stratigraphy in well logs, core, and outcrops: concepts for high–resolution correlation of time and facies," *AAPG Methods in Exploration Series*, vol. 7, p. 55, 1990.

[3] P. R. Vail, F. Audemard, S. A. Bowman, and P. N. Eisner, "The stratigraphic signatures of tectonics, eustasy and sedimentology–an overview," in *Cycles and Events in Stratigraphy*, G. Einsele, W. Ricken, and A. Seilacher, Eds., pp. 617–659, Springer–Verlag, Berlin, 1991.

[4] O. Catuneanu, V. Abreu, J. P. Bhattacharya et al., "Towards the standardization of sequence stratigraphy," *Earth-Science Reviews*, vol. 92, no. 1–2, pp. 1–33, 2009.

[5] J. Wu and Z. X. Jiang, "Division and characteristics of shale parasequences in the upper fourth member of the Shahejie Formation, Dongying Depression, Bohai Bay Basin, China," *Journal of Earth Science*, vol. 28, no. 6, pp. 1006–1019, 2017.

[6] R. B. Ainsworth, J. B. McArthur, S. C. Lang, and A. J. Vonk, "Quantitative sequence stratigraphy," *AAPG Bulletin*, vol. 102, no. 10, pp. 1913–1939, 2018.

[7] S. Wang, L. Y. Shao, D. D. Wang, Q. P. Sun, B. Sun, and J. Lu, "Sequence stratigraphy and coal accumulation of Lower Cretaceous coal-bearing series in Erlian Basin, northeastern China," *AAPG Bulletin*, vol. 103, no. 7, pp. 1653–1690, 2019.

[8] M. G. Smith and R. M. Bustin, "Late Devonian and Early Mississippian Bakken and Exshaw black shale source rocks, Western Canada sedimentary basin: a sequence stratigraphic interpretation," *AAPG Bulletin*, vol. 84, pp. 940–960, 2000.

[9] S. Angulo and L. A. Buatois, "Integrating depositional models, ichnology, and sequence stratigraphy in reservoir characterization: the middle member of the Devonian-Carboniferous Bakken Formation of subsurface southeastern Saskatchewan revisited," *AAPG Bulletin*, vol. 96, no. 6, pp. 1017–1043, 2012.

[10] T. J. Algeo, L. Schwark, and J. C. Hower, "High-resolution geochemistry and sequence stratigraphy of the Hushpuckney Shale (Swope Formation, eastern Kansas): implications for climato- environmental dynamics of the Late Pennsylvanian Midcontinent Seaway," *Chemical Geology*, vol. 206, no. 3-4, pp. 259–288, 2004.

[11] R. M. Slatt and N. D. Rodriguez, "Comparative sequence stratigraphy and organic geochemistry of gas shales: commonality or coincidence?," *Journal of Natural Gas Science and Engineering*, vol. 8, pp. 68–84, 2012.

[12] F. R. Ettensohn, L. P. Fulton, and R. C. Kepferle, "Use of scintillometer and gamma-ray logs for correlation and stratigraphy in homogeneous black shales," *Geological Society of America Bulletin*, vol. 90, no. 5_Part_II, pp. 828–849, 1979.

[13] M. O. Abouelresh and R. M. Slatt, "Lithofacies and sequence stratigraphy of the Barnett Shale in east-central Fort Worth Basin, Texas," *AAPG Bulletin*, vol. 96, no. 1, pp. 1–22, 2012.

[14] Z. X. Jiang, C. Liang, J. Wu et al., "Several issues in sedimentological studies on hydrocarbon-bearing fine-grained sedimentary rocks," *Acta Petrolei Sinica*, vol. 34, pp. 1031–1039, 2013.

[15] Y. Q. Ma, M. J. Fan, Y. C. Lu et al., "Climate-driven paleolimnological change controls lacustrine mudstone depositional process and organic matter accumulation: constraints from lithofacies and geochemical studies in the Zhanhua Depression, eastern China," *International Journal of Coal Geology*, vol. 167, pp. 103–118, 2016.

[16] C. Liang, J. Wu, Z. X. Jiang, Y. C. Cao, S. J. Liu, and S. Y. Feng, "Significances of organic matters on shale deposition diagenesis process and reservoir formation," *Journal of China University of Petroleum*, vol. 41, pp. 1–8, 2017.

[17] R. G. Loucks, R. M. Reed, S. C. Ruppel, and D. M. Jarvie, "Morphology, genesis, and distribution of nanometer-scale pores in siliceous mudstones of the Mississippian Barnett Shale," *Journal of Sedimentary Research*, vol. 79, no. 12, pp. 848–861, 2009.

[18] C. Liang, Y. Cao, K. Liu, Z. Jiang, J. Wu, and F. Hao, "Diagenetic variation at the lamina scale in lacustrine organic-rich shales: implications for hydrocarbon migration and accumulation," *Geochimica et Cosmochimica Acta*, vol. 229, pp. 112–128, 2018.

[19] H. M. Liu, S. Zhang, G. Q. Song et al., "A discussion on the origin of shale reservoir inter-laminar fractures in the Shahejie Formation of Paleogene, Dongying Depression," *Journal of Earth Science*, vol. 28, no. 6, pp. 1064–1077, 2017.

[20] Z. Li, Y. R. Zou, X. Y. Xu, J. N. Sun, M. W. Li, and P. A. Peng, "Adsorption of mudstone source rock for shale oil - experiments, model and a case study," *Organic Geochemistry*, vol. 92, pp. 55–62, 2016.

[21] C. Liang, Y. Cao, Z. Jiang, J. Wu, S. Guoqi, and Y. Wang, "Shale oil potential of lacustrine black shale in the Eocene Dongying Depression: implications for geochemistry and reservoir characteristics," *AAPG Bulletin*, vol. 101, no. 11, pp. 1835–1858, 2017.

[22] X. Guo, K. Liu, S. He et al., "Petroleum generation and charge history of the northern Dongying Depression, Bohai Bay Basin, China: insight from integrated fluid inclusion analysis and basin modelling," *Marine and Petroleum Geology*, vol. 32, no. 1, pp. 21–35, 2012.

[23] J. Wang, Y. C. Cao, J. Xiao, K. Y. Liu, and M. S. Song, "Factors controlling reservoir properties and hydrocarbon accumulation of the Eocene lacustrine beach-bar sandstones in the Dongying Depression, Bohai Bay Basin, China," *Marine and Petroleum Geology*, vol. 99, pp. 1–16, 2019.

[24] Y. Q. Ma, M. J. Fan, Y. C. Lu, H. M. Liu, S. P. Zhang, and X. F. Liu, "Stable isotope record of middle Eocene summer monsoon and its instability in eastern China," *Global and Planetary Change*, vol. 175, pp. 103–112, 2019.

[25] Z. X. Jiang, J. H. Wang, C. S. Fulthorpe, L. A. Liu, Y. F. Zhang, and H. M. Liu, "A quantitative model of paleowind reconstruction using subsurface lacustrine longshore bar deposits - an attempt," *Sedimentary Geology*, vol. 371, pp. 1–15, 2018.

[26] G. G. Lash and D. R. Blood, "Organic matter accumulation, redox, and diagenetic history of the Marcellus Formation, southwestern Pennsylvania, Appalachian Basin," *Marine and Petroleum Geology*, vol. 57, no. 57, pp. 244–263, 2014.

[27] C. Liang, J. Wu, Z. Jiang, Y. Cao, and G. Q. Song, "Sedimentary environmental controls on petrology and organic matter accumulation in the upper fourth member of the Shahejie Formation (Paleogene, Dongying Depression, Bohai Bay Basin, China)," *International Journal of Coal Geology*, vol. 186, pp. 1–13, 2018.

[28] B. Jones and D. A. Manning, "Comparison of geochemical indices used for the interpretation of palaeoredox conditions in ancient mudstones," *Chemical Geology*, vol. 111, no. 1–4, pp. 111–129, 1994.

[29] Q. Li, S. H. Wu, D. L. Xia, X. L. You, H. M. Zhang, and H. Lu, "Major and trace element geochemistry of the lacustrine organic-rich shales from the Upper Triassic Chang 7 member in the southwestern Ordos Basin, China: implications for paleoenvironment and organic matter accumulation," *Marine and Petroleum Geology*, vol. 111, pp. 852–867, 2020.

[30] T. W. Lyons, J. P. Werne, D. J. Hollander, and R. W. Murray, "Contrasting sulfur geochemistry and Fe/Al and Mo/Al ratios across the last oxic-to-anoxic transition in the Cariaco Basin, Venezuela," *Chemical Geology*, vol. 195, no. 1-4, pp. 131–157, 2003.

[31] T. F. Pedersen and S. E. Calvert, "Anoxia vs. productivity: what controls the formation of organic-carbon-rich sediments and sedimentary rocks," *Aapg Bulletin*, vol. 74, pp. 454–466, 1990.

[32] M. L. Caplan and R. M. Bustin, "Palaeoceanographic controls on geochemical characteristics of organic-rich Exshaw mudrocks: role of enhanced primary production," *Organic Geochemistry*, vol. 30, no. 2-3, pp. 161–188, 1999.

[33] M. A. Arthur and B. B. Sageman, "Marine black shales: depositional mechanisms and environments of ancient deposits," *Annual Reviews of Earth and Planetary Sciences*, vol. 22, no. 1, pp. 499–551, 1994.

[34] J. Wu, C. Liang, Z. Q. Hu et al., "Sedimentation mechanisms and enrichment of organic matter in the Ordovician Wufeng Formation-Silurian Longmaxi Formation in the Sichuan Basin," *Marine and Petroleum Geology*, vol. 101, pp. 556–565, 2019.

[35] C. Liang, Z. Jiang, Y. Cao, J. Wu, Y. Wang, and H. Fang, "Sedimentary characteristics and origin of lacustrine organic–rich shales in the salinized Eocene Dongying Depression," *GSA Bulletin*, vol. 130, no. 1-2, pp. 154–174, 2018.

[36] M. Mastalerz, A. Drobniak, and A. B. Stankiewicz, "Origin, properties, and implications of solid bitumen in source-rock reservoirs: a review," *International Journal of Coal Geology*, vol. 195, pp. 14–36, 2018.

[37] J. Wu, C. Liang, R. C. Yang, and J. Xie, "The significance of organic matter-mineral associations in different lithofacies in the Wufeng and Longmaxi shale-gas reservoirs in the Sichuan Basin," *Marine and Petroleum Geology*, vol. 126, p. 104866, 2021.

[38] D. A. V. Stow, A. Y. Hue, and P. Bertrand, "Depositional processes of black shales in deep water," *Marine and Petroleum Geology*, vol. 18, no. 4, pp. 491–498, 2001.

[39] S. J. Han, B. S. Yu, C. Y. Bai, M. E. Na, Z. H. Shen, and J. J. Guo, "Microbial sedimentation of Shahejie Formation micritic carbonate in the Dongying Depression, Bohai Bay Basin," *Journal of Mineralogy and Petrology*, vol. 38, pp. 104–113, 2018.

[40] S. Q. Liu, Z. X. Jiang, Y. B. He et al., "Geomorphology, lithofacies and sedimentary environment of lacustrine carbonates in the Eocene Dongying Depression, Bohai Bay Basin, China," *Marine and Petroleum Geology*, vol. 113, p. 104125, 2020.

[41] E. Flügel, *Microfacies of Carbonate Rocks: Analysis, Interpretation and Application*, Springer-Verlag, Berlin Heidelberg, 2010.